Numerical study of interface reconstruction method in under-resolved regions of the flow for liquid jet primary breakup

Anirudh Asuri Mukundan, T. Menard, A. Berlemont, Jorge César Brändle de Motta

Numerical study of interface reconstruction method in under-resolved regions of the flow for liquid jet primary breakup

A. Asuri Mukundan*, T. Ménard, A. Berlemont, J. C. Brändle de Motta
CNRS UMR6614–CORIA & Université de Rouen Normandie, Saint Étienne du Rouvray, Rouen, France
anirudh.mukundan@coria.fr, thibaut.menard@coria.fr, alain.berlemont@coria.fr, and jorge.brandle@coria.fr

Abstract

Liquid/gas interface reconstruction continues to be a challenge in the numerical study of liquid fuel atomization. This paper focuses on one such reconstruction method called moment of fluid (MOF) method intended specifically for interface reconstruction in under-resolved flow regions. MOF method gives two-fold advantage over volume of fluid (VOF), level set (LS), and coupled level set volume of fluid (CLSVOF), such as: first, MOF preserves the shape and orientation of interfaces that are commonly encountered in under-resolved regions of the flow, and second, it exhibits second-order accuracy in spatial resolution for multiple interface topologies. For various test cases considered in this paper, MOF has consistently proved to be more accurate than and at least as accurate as CLSVOF method.

Keywords: multiphase, moment of fluid, center of mass, volume fraction

---

Introduction

Atomization of injected liquid fuel in gas turbines and internal combustion (IC) engines play a major role in the production of harmful pollutant emissions. This is due to the fact that the efficiency of liquid fuel combustion and production of pollutants has a direct dependency on the mixing between fuel and oxidizer, which in itself results from the cascade of the mechanisms initiated by the process of atomization of injected liquid fuel stream. Due to the multiphase characteristic and multi-physical aspect of the liquid fuel atomization, and often due to the presence of highly turbulent environment, experimental investigations proves to be a challenging endeavor. This motivates the need for the development of numerical methods to study the atomization process.

An obvious requirement of these methods is least numerical error which will make it more trustable and suitable to be used in detailed simulations such as direct numerical simulations (DNS) of liquid atomization [1–3]. In addition, these numerical methods ideally must require less computational resources, thus not taxing even the most powerful supercomputers available today [4].

In the presence of complex topological structures encountered in liquid fuel atomization, the underlying equations are stiff, thus the development and improvement of numerical methods to treat such structures has been an active area of research. Of the many sharp interface reconstruction methods, volume of fluid (VOF) method [5–9], level set (LS) method [10–14], and their variant such as coupled level set volume of fluid (CLSVOF) method [1, 3, 15] have been proved to perform well on variety of canonical test cases. Although these validated methods prove to be successful in multiple applications, the geometrical property computations can still be inaccurate especially in the under-resolved regions of the flow. This results from the inaccurate computation of unit normal of the interface in such regions. To mitigate this inaccuracy, a numerical interface reconstruction method called moment of fluid (MOF) method [16] is developed in the in-house code ARCHER [1, 10, 17] and presented in this work. MOF method has been proved – to preserve the orientation of the liquid/gas interface in the context of multiphase flows [16, 18]; to be second-order accurate in spatial resolution [19].

The objectives of this paper are: to present MOF method for interface reconstruction in the context of incompressible multiphase flows as a potential interface tracking technique, compare and contrast the results of interface reconstruction for various academic test cases between MOF and CLSVOF methods, and to emphasize the relevance of the usage of the MOF method especially in the under-resolved regions flow regions.

Moment of Fluid (MOF) method

MOF method is an extension of VOF method for interface tracking in the context of multiphase flows. VOF method uses only liquid volume fraction F (0^{th} moment of the liquid volume) for tracking the interface in every

*Corresponding author: anirudh.mukundan@coria.fr

mixed computational cell. As a step further, MOF method tracks both the liquid volume fraction and coordinates of the liquid center of mass (COM) $\underline{x}_{\mathrm{COM}}$ (1^{st} moment of liquid volume) for the interface reconstruction in each such cell. A mixed computational cell, within this study, is defined as the cell in which $0 < F < 1$ holds. The definitions of the 0^{th} and 1^{st} moments of the liquid volume are given as

$$F = \frac{\int_\omega d\underline{x}}{\int_\Omega d\underline{x}}, \tag{1}$$

$$\underline{x}_{\mathrm{COM}} = \frac{\int_\omega \underline{x} d\underline{x}}{\int_\Omega d\underline{x}}, \tag{2}$$

where ω is the domain of the liquid packet inside the computational cell Ω. The availability of these two parameters establishes a self-sufficiency of the required information to reconstruct the approximate interface in a cell thus, eradicating data requirement from its neigbours. This results in a uniform treatment of the internal and boundary cells in the mesh thus, yielding the resolution of the interface as high as that of the computational mesh itself. Within this work, the MOF method is developed in the in-house code ARCHER.

Interface Reconstruction

The commonly used piecewise linear interface calculation (PLIC) is employed in this work for approximating the original interface. Thus, the equation of the approximated interface in 3D is given by $ax + by + cz + d = 0$, which represents the equation of a plane. In 2D, this equation becomes the equation of a line. The unit normal $\underline{n}$ of the interface is therefore expressed as $n = [a,\ b,\ c]^T$. The shortest distance of the interface from the cell center is characterized by the parameter d.

The interface reconstruction in MOF method is a constrained optimisation problem as described in [18] wherein $\underline{n}$ and d have to be determined simultaneously by the satisfaction of the two conditions

$$\mid F^{\mathrm{ref}} - F^{\mathrm{act}}(\underline{n}, d) \mid = 0, \text{ and} \tag{3}$$

$$E^{\mathrm{MOF}}(\underline{n}, d) = \min_{\text{Eq. (3) holds}} \left\| \underline{x}^{\mathrm{ref}}_{\mathrm{COM}} - \underline{x}^{\mathrm{act}}_{\mathrm{COM}}(\underline{n}, d) \right\|_2 . \tag{4}$$

All the variables containing the superscript "ref" represents the variables pertaining to the original (reference) interface while those containing the superscript "act" represents the variables pertaining to the reconstructed (actual) interface. The explanation of these conditions is assisted through Figure 1. The shortest distance of the interface

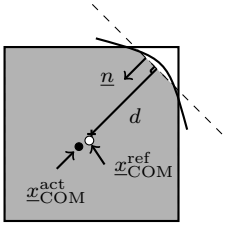

Figure 1: Mathematical Representation of MOF method

from the cell center d is determined by the volume conservation condition Equation (3). To this end, the linear approximated interface (shown by dashed line in Figure 1) is constructed such that the volume of liquid is exactly the same under reference (shown by solid line in Figure 1) and actual interface upto the machine precision. The computation of optimal value of d is carried out using Newton-Raphson iterative method as described in Ménard et al [1]. The interface unit normal is then computed by minimising the error E^{MOF} (also called distance defect) between the coordinates of the reference and the acutal COM of the liquid in the computational cell (c.f. Equation (4)).

In order to solve this minimisation problem, $\underline{n}$ is parameterised [18] using the polar coordinates as follows

$$\underline{n} = \begin{bmatrix} a \\ b \\ c \end{bmatrix} = \begin{bmatrix} \sin\Phi\cos\Theta \\ \sin\Phi\sin\Theta \\ \cos\Phi \end{bmatrix} . \tag{5}$$

Thus, the Equation (4) transforms into a non-linear least square problem for (Φ, Θ), i.e., finding (Φ^*, Θ^*) such that the error E^{MOF} is minimum, i.e.,

$$E^{\mathrm{MOF}}(\underline{n}, d) = \left\|\underline{g}(\Phi^*, \Theta^*, d)\right\|_2 = \min_{\text{Eq.(3) holds}} \left\|\underline{g}(\Phi, \Theta, d)\right\|_2, \tag{6}$$

where $\underline{g}(\Phi, \Theta, d) = \underline{x}^{\mathrm{ref}}_{\mathrm{COM}} - \underline{x}^{\mathrm{act}}_{\mathrm{COM}}$. Equation (6) is solved numerically for (Φ^*, Θ^*) using Gauss-Newton method. Once the optimal parametric angles (Φ^*, Θ^*) are known, the components of the unit normal $[a, b, c]^T$ can be retrieved using Equation (5). The new reference COM in each cell takes the value of the acutal COM pertaining to the reconstructed interface using which the new values of the normal components are computed.

Interface Advection

The advection of interface in the case of MOF method involves advection of both reference liquid volume fraction F^{ref} and coordinates of reference COM $\underline{x}^{\mathrm{ref}}_{\mathrm{COM}}$. A directionally split numerical scheme is employed for the advection of both quantities. The transport equation and numerical scheme implemented for the advection are presented in the following subsections. Since the advection pertains solely to the reference quantities, the superscript "ref" will be dropped in volume fraction and the coordinates of the COM hereon.

Volume Fraction

The advection equation for the volume fraction solved in ARCHER is given as

$$\frac{\partial F}{\partial t} + \nabla \cdot (F\underline{u}) = c\,(\nabla \cdot \underline{u}); \quad c = \begin{cases} 1, & F > 0.5 \\ 0, & \text{otherwise} \end{cases} \tag{7}$$

The algorithm proposed in the work of Weymouth and Yue [20] is implemented for the advection of the volume fraction. For more details on the finite difference discretization of the above equation and computation of volume fluxes across cell faces, the reader is referred to [20].

Centre of Mass

The advection equation of the reference COM is given as

$$\frac{d}{dt}(\underline{x}_{\mathrm{COM}}) = \underline{u}(\underline{x}_{\mathrm{COM}}), \tag{8}$$

where $\underline{u}(\underline{x}_{\mathrm{COM}})$ is the velocity field interpolated linearly from the face-centers of the computational cell to the location of the COM. This velocity is non-dimensionalized using the mesh spacing and the time step size $\Delta t = t^{n+1} - t^n$, hence the velocity component becomes the local Courant-Friedrichs-Lewy (CFL) number. In this study, the COM is considered as a Lagrangian particle [16, Appendix A] that is associated with a liquid packet/parcel.

An Eulerian Implicit–Lagrangian Explicit (EI–LE) scheme [21] is employed in this study for solving Equation (8). A first order integration scheme of this equation keeping constant velocity over the time step size Δt yields,

$$\underline{x}^{n+1}_{\mathrm{COM}} = \underline{x}^{n}_{\mathrm{COM}} + u(\underline{x}^{*}_{\mathrm{COM}}) \tag{9}$$

in which the mode of the scheme is Eulerian Implicit if $\underline{x}^{*}_{\mathrm{COM}} = \underline{x}^{n+1}_{\mathrm{COM}}$ and Lagrangian Explicit if $\underline{x}^{*}_{\mathrm{COM}} = \underline{x}^{n}_{\mathrm{COM}}$. In order to have the consistency between the advection of liquid volume fraction and COM, the mode of the scheme for COM advection is switched between EI and LE for a Cartesian direction at each time step, i.e., if $x-$direction advection of COM for $t^n \rightarrow t^{n+1}$ is carried out using EI mode, then the $x-$direction advection of COM for $t^{n+1} \rightarrow t^{n+2}$ will be carried out in LE mode.

In this study, the coupling between the advections of the volume fraction and that of COM is carried out similar to that in the study of Jemison et al [18].

Results and Discussion

In this section, the accuracy, order of convergence, and utility of the MOF interface reconstruction method are analyzed using different canonical test cases. The choices of the validation tests considered in this study are made so that the errors due to reconstruction and advection algorithms used in this study can be assessed. In each of the presented tests, the reconstruction accuracy of MOF and CLSVOF algorithms are compared along with the order of convergence of the error with respect to the spatial resolution of the mesh.

Since the advection errors are almost always accompanied with the reconstruction errors, these errors are reported and addressed using separate test cases for better evaluation of the performance of the reconstruction and advection algorithm implemented in this study. In all the test cases presented in this work, a constant CFL number of 0.5, periodic boundary conditions along $x-$ and $y-$directions, and $\Delta x = \Delta y = \text{const.}$ are used. The time step size Δt is computed from the CFL number and the mesh spacing.

Translation test

Following the work of Harvie and Fletcher [22], the advection of circular liquid droplet of radius $r = 0.25$ units placed at the center of a 1×1 domain is considered for analysing the errors due to reconstruction from MOF and CLSVOF methods. The CLSVOF method developed by Ménard et al [1] is used in this study for the comparison of results with MOF method. The advection is performed along $x-$direction with unit velocity such that the interface crosses the boundary and comes back to the same initial location at the final time step. Since the velocity is uniform, obeys continuity equation and does not have any gradient in the domain, the errors arising at the end of advection is purely from the reconstruction algorithm. This error is computed as

$$E = \sum_{i,j} A_{ij} \mid F_{i,j}^{nT} - F_{i,j}^{0} \mid, \tag{10}$$

where $A_{i,j}$ is the area of the cell, F^0 and F^{nT} are the liquid volume fractions at the initial and final time iteration instants respectively. The mesh resolutions considered in this test are 16×16, 32×32, 64×64, 128×128, and 256×256. Figure 2 shows the initial interface (black line) and final interfaces (red line: MOF in left subfigure,

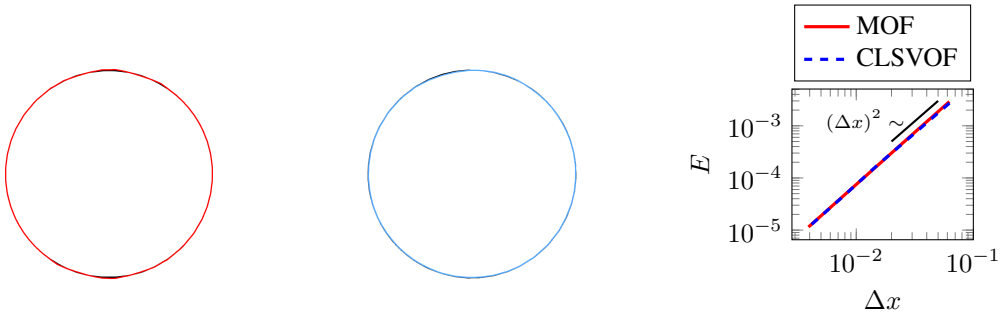

(a) MOF (b) CLSVOF (c) Error convergence for circle translation

Figure 2: 32×32 mesh; Black line ($nt = 0$): Initial; Red line ($nt = 128$): MOF; Blue line ($nt = 128$): CLSVOF

blue line: CLSVOF in middle subfigure) of the circular liquid droplet after the advection for 32×32 mesh. The circle comes back to its initial location after 128 time advancement iterations for this mesh resolution. For such interface topology, it can be seen qualitatively that both MOF and CLSVOF methods have performed well. From the error convergence plot shown in Figure 2c, it is quite obvious that both MOF and CLSVOF display second-order convergence rate.

Rotation Test

The same case as described in Rider and Kothe [23] is considered in which a circle of radius $r = 0.15$ units is placed in a 1×1 domain with center at $(0.5, 0.75)$, rotates around the center of the domain in a spatially varying field given by

$$u = \frac{\pi}{3.14}(0.5 - y), \text{ and} \tag{11}$$

$$v = \frac{\pi}{3.14}(x - 0.5). \tag{12}$$

In the exact solution, the circle retains its shape thus, this test assesses the efficiency of the EI–LE advection algorithm implemented in this study. The error in the numerical solution is computed using Equation (10) where nT is the final time iteration at which the interface completes one full revolution around the center of the domain. The results of the error for the mesh resolutions 32×32, 64×64, and 128×128 are presented and compared in the Figure 3 for MOF and CLSVOF reconstruction algorithms. The initial interface is depicted by black line, the final interfaces from MOF and CLSVOF reconstruction methods are depicted by red and blue lines respectively.

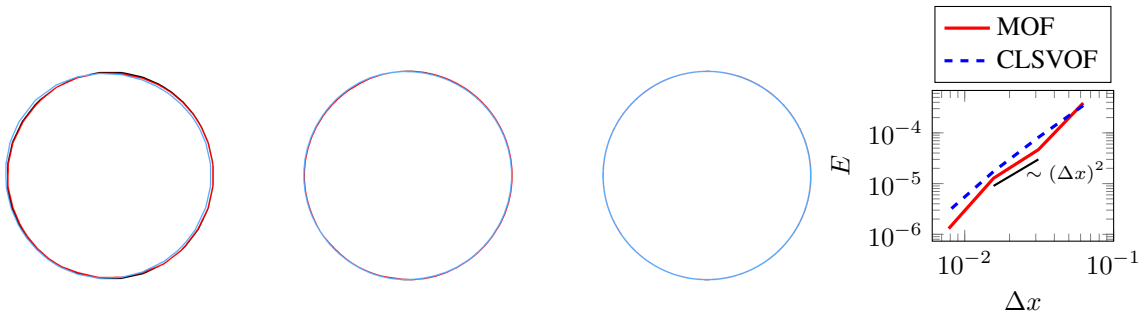

(a) 32×32 (b) 64×64 (c) 128×128 (d) Error convergence for circle rotation

Figure 3: Initial and final interfaces of circle after one full rotation and error convergence plot

It can be observed from this figure that for such a simple advection problem, the advection schemes employed for the volume fraction and COM in this study for MOF method is qualitatively more accurate than CLSVOF method. Furthermore, from Figure 3d for mesh resolutions from 16×16 to 128×128, it is observed that MOF method exhibits second-order convergence rate and produces lower error than CLSVOF method.

Zalesak's notched disk test

In this test, a slotted circle of fluid rotates around the center of the domain in a solenoidal velocity field. This test is indeed an assessment of the efficiency of the reconstruction algorithm than that of the advection algorithm.

Within this test, a slotted circle of radius $r = 0.15$ units having slot width of 0.06 units and slot length of 0.2 units is placed in a 1×1 domain with center of the circle located at $(0.5, 0.75)$. The rotation of this slotted circle is accomplished using velocity fields given in the Equations (11) and (12). Since this velocity is divergence-free throughout the domain, the interface of the Zalesak's notched circular disk is expected to retain the original shape at the end of rotation. The test ends when the first (anticlockwise) revolution of the slotted circular disk is completed. The resulting error between the exact and the reconstructed interface is then computed as

$$E = \frac{\sum_{i,j} \mid F_{i,j}^{nT} - F_{i,j}^{0} \mid}{\sum_{i,j} \mid F_{i,j}^{0} \mid}, \tag{13}$$

where the definitions of F^0 and F^{nT} remains the same as explained in the previous subsection. The results from this test are shown in Figure 4 for 32×32, 64×64, and 128×128 mesh resolutions. The initial interface is depicted using black solid line, the final interface from MOF algorithm is depicted using red solid line while that from CLSVOF algorithm is depicted using blue solid line.

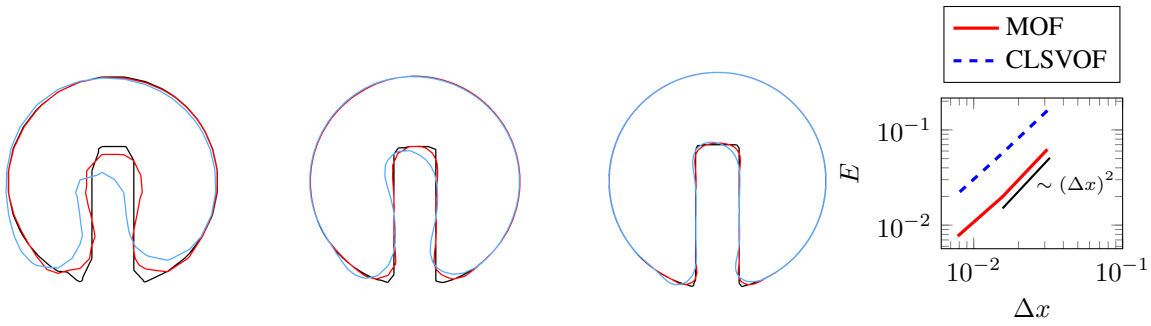

(a) 32×32 (b) 64×64 (c) 128×128 (d) Error convergence for Zalesak disk rotation

Figure 4: Initial and final interface of Zalesak's slotted disk after one full revolution and error convergence plot

It can be observed from Figures 4a to 4c, that the error in reconstruction is mainly concentrated in the regions of high curvature of the interface. Furthermore, it is obvious from from Figure 4d that the MOF method is

quantitatively more accurate in capturing the interface under a solenoidal velocity field than CLSVOF method.

Vortex in a box test

This test assesses the ability of an interface reconstruction method to represent the under-resolved structures such as ligaments in a robust manner. In this test, a circular disk is made to undergo high amount of deformation under a given velocity field. The following time reversing velocity field is prescribed over the whole 1×1 domain

$$u = -2\sin^2(\pi x)\sin(\pi y)\cos(\pi y)\cos(\pi t/T) \tag{14}$$

$$v = 2\sin^2(\pi y)\sin(\pi x)\cos(\pi x)\cos(\pi t/T) \tag{15}$$

where T is the time period of reversal of the velocity field. In this study, $T = 6$ is chosen for the analysis of the interface reconstruction accuracy. This velocity field stretches and tears the initially circular fluid body as it becomes progressively entrained by the vortex and comes back to its original shape at time $t = T$. The entrainment is demonstrated as long thin fluid filament spiraling inward towards the vortex center. Unlike Zalesak's notched disk test, the velocity field in this test is non-linear deeming this test to be a more realistic assessment for the reconstruction method.

The results of the interfaces are shown in Figure 5 for the mesh resolutions 64×64, 128×128, and 256×256 with the reference solution (depicted by black solid line in the subfigures) obtained on a 1024×1024 grid. The top row in this figure pertain to the time instant $t = T/2$ corresponding to the maximum stretching of the fluid body and those at the bottom row pertain to the time instant $t = T$ corresponding to the return to the original shape. The

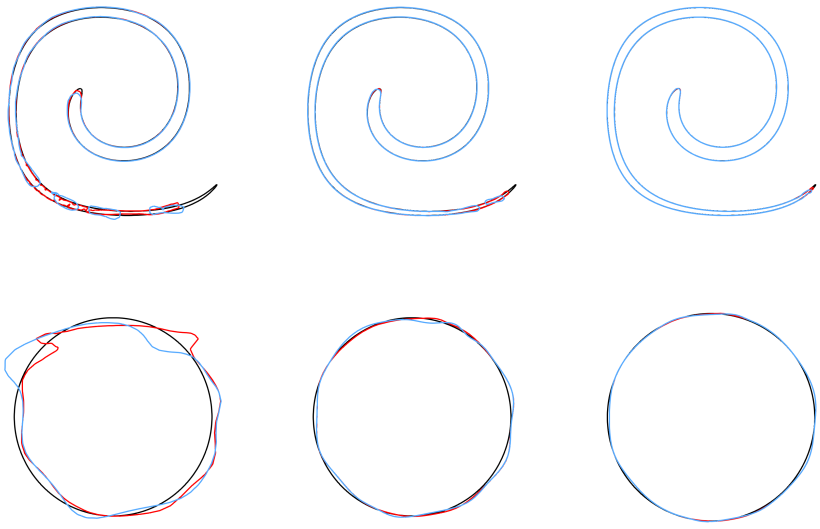

(a) 64×64 (b) 128×128 (c) 256×256

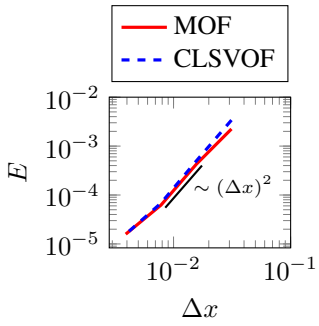

(d) Error convergence for vortex in a box test

Figure 5: Vortex in a box test; $t = T/2$ (top row) and $t = T$ (bottom row) and error convergence plot

reconstruction algorithm proves to be robust in the smooth regions of the interface and it can be said qualitatively that the results become better with the increase in mesh resolution at both the time instants of maximum stretch and at final time instant at which the interface returns back to its original shape. Figure 5d quantifies the reconstruction error computed at time $t = T$ when the interface returns to its initial shape. This error is computed according to Equation (10). From this figure, it can be seen that both MOF and CLSVOF reconstruction algorithms are of the same level of accuracy in terms of reconstruction error. Once again, it can be seen that the MOF method exhibit second-order accuracy in spatial resolution.

Deformation of circular fluid body test

A complex time reversing velocity field [24] given by

$$u = \sin(4\pi(x + 1/2))\sin(4\pi(y + 1/2))\cos(\pi t/T) \tag{16}$$

$$v = \cos(4\pi(x + 1/2))\cos(4\pi(y + 1/2))\cos(\pi t/T) \tag{17}$$

is used in this test for the deformation of a circular bubble under extreme conditions. This velocity field will induce radical deformation in the topology of the fluid body thereby providing a more stringent test for the reconstruction method than those presented before. To this end, a circular fluid body of radius $r = 0.15$ units is placed with its center at $(0.5, 0.75)$ in a 1×1 domain. At its maximum deformation, the circular fluid body is entrained into two of the four nearest vortices with a small portion (thin filaments) entrapped by the two of the nearby vortices. The time period for velocity reversal is chosen as $T = 2.0$ for this test.

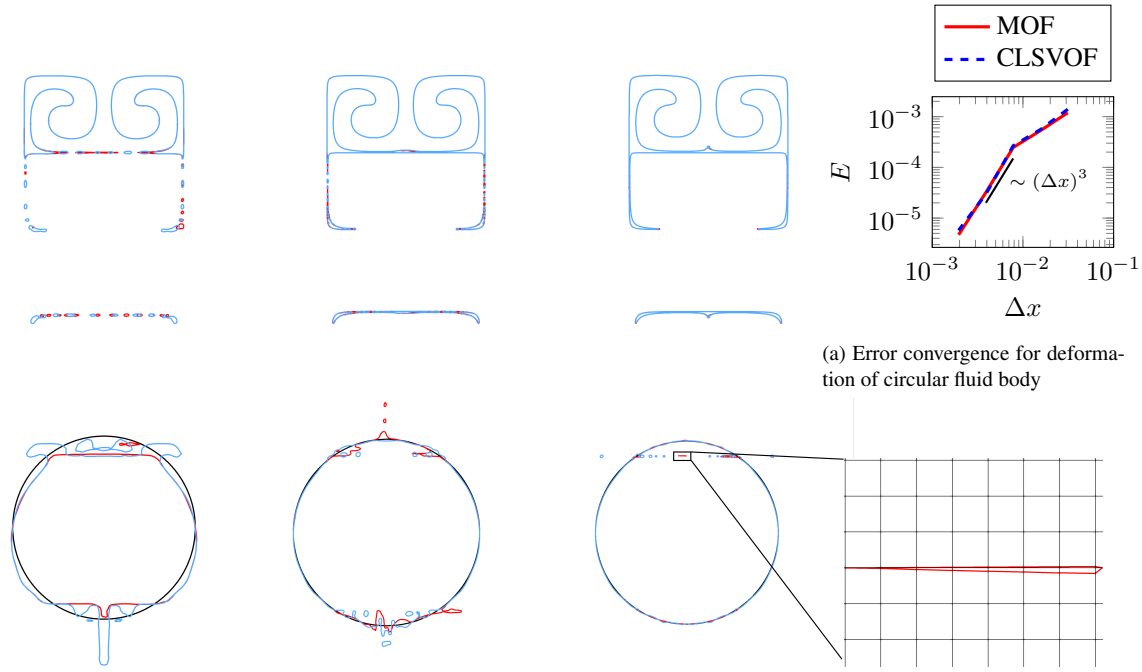

(a) Error convergence for deformation of circular fluid body

(b) 128×128 (c) 256×256 (d) 512×512

Figure 6: Interface reconstruction for deformation of circular fluid body $t = T/2$ (top row) and $t = T$ (bottom row) and error convergence plot

The results are shown in Figures 6b to 6d for the 128×128, 256×256, and 512×512 mesh resolutions for $t = T/2$ (top row) and $t = T$ (bottom row) with initial interface (black line), reconstructed interfaces using MOF (red line), and CLSVOF (blue line) for the corresponding time instants. In addition, a zoomed view of the miniature ligament is found in the final time iteration of the 512×512 mesh is shown. From this zoomed view along with the underlying mesh, it can be seen that the depicted interface structure is extremely under-resolved. Thus, even with MOF method spurious oscillations in the final interface are seen in the figures in the top row of Figures 6b to 6d. Albeit this current limitation, even under extreme velocity fields which is tearing the interface apart, the MOF is observed to perform satisfactorily for interface reconstruction under extreme deformations of the liquid body topology (c.f. top row in Figures 6b to 6d).

The error from the reconstruction method is quantified using the Equation (10). The plot of the convergence of this error for 32×32, 64×64, 128×128, 256×256, and 512×512 mesh resolutions is shown in Figure 6a. It can be seen that the MOF method is performing to a satisfactory extent for any mesh resolution considered in this test case considering the fact that the interface is entirely deformed due to the prescribed velocity field. Furthemore, it can be seen that both the MOF and CLSVOF method exhibits a third-order convergence rate for all the spatial resolutions considered for this test case. The reason for this behavior in comparison to the other test cases could be attributed to the fact that as the mesh resolution increases, particularly for this test case, smaller structures of the interface are increasingly identified thereby enhancing the convergence rate of the error.

Conclusions

Study of liquid fuel atomization process is essential in order to meet the stringent emission norms. This is due to the fact that this process has a direct influence on the pollutant emissions. Numerical study of atomization under turbulent conditions gives insights which are otherwise challenging to obtain through experimental investigatations.

Within this work, MOF method was presented for reconstruction of liquid/gas interface in the context of incompressible multiphase flows to the application of numerical analysis of primary breakup of liquid fuel. This method involves computation of interface unit normal by reducing the defect in the first order moment of liquid volume in a volume conservative manner. For various test cases presented in this study, MOF method proved to be more accurate than and at least as accurate as that of CLSVOF method in terms of reconstruction error and preservation of the shape and orientation of the interface topologies. Furthermore, MOF method demonstrated its superior capability of preserving the interface for topologies found in under-resolved flow structures such as thin filaments and ligaments. This deems MOF method as an interface reconstruction method to be used in DNS for studying primary atomization.

In future, development of a hybrid MOF–CLSVOF method for interface reconstruction is a promising improvement thereby combining the advantages of both methods for interface reconstruction. MOF method requires more computational resources than CLSVOF method for the interface reconstruction mainly due to its unit normal computation from the COM. Thus, it is more prudent to use CLSVOF for interface reconstruction especially for the topologies that are far less complicated making it more sensible to develop a hybrid MOF–CLSVOF method. Also, the volume fraction and COM of gas phase along with those pertaining to the liquid phase should be considered for optimal interface reconstruction in the next studies.

Acknowledgements

The funding for this project from the European Union's Horizon 2020 research and innovation programme under the Marie Skłodowska-Curie grant agreement No. 675676 is gratefully acknowledged.

References

[1] Ménard, T., Tanguy, S., and Berlemont, A. *International Journal of Multiphase Flow* 33(5):510–524 (2007).
[2] Desjardins, O. and Pitsch, H. *Atomization and Sprays* 20(4):311–336 (2010).
[3] Le Chenadec, V. and Pitsch, H. *Atomization and Sprays* 23(12):1139–1165 (2013).
[4] Gorokhovski, M. and Herrmann, M. *Annual Review of Fluid Mechanics* 40:343–366 (2008).
[5] Aulisa, E., Manservisi, S., Scardovelli, R., and Zaleski, S. *Journal of Computational Physics* 192(1):355–364 (2003).
[6] López, J., Zanzi, C., Gómez, P., Faura, F., and Hernández, J. *International Journal for Numerical Methods in Fluids* 58(8):923–944 (2008).
[7] Hernández, J., López, J., Gómez, P., Zanzi, C., and Faura, F. *International Journal for Numerical Methods in Fluids* 58:897–921 (2008).
[8] Aniszewski, W., Ménard, T., and Marek, M. *Computers & Fluids* 97:52–73 (2014).
[9] Owkes, M. and Desjardins, O. *Journal of Computational Physics* 332:21–46 (2017).
[10] Tanguy, S. and Berlemont, A. *International Journal of Multiphase Flow* 31:1015–1035 (2005).
[11] Desjardins, O., Moureau, V., and Pitsch, H. *Journal of Computational Physics* 227:8395–8416 (2008).
[12] Herrmann, M. *Journal of Computational Physics* 227:2674–2706 (2008).
[13] Herrmann, M. *Atomization and Sprays* 21(4):283–301 (2011).
[14] Shinjo, J. and Umemura, A. *International Journal of Multiphase Flow* 37:1294–1304 (2011).
[15] Le Chenadec, V. and Pitsch, H. *Journal of Computational Physics* 233:10–33 (2013).
[16] Dyadechko, V. and Shashkov, M. *Journal of Computational Physics* 227:5361–5384 (2008).
[17] Vaudor, G., Ménard, T., Aniszewski, W., Doring, M., and Berlemont, A. *Computers and Fluids* 152:204–216 (2017).
[18] Jemison, M., Loch, E., Sussman, M., Shashkov, M., Arienti, M., Ohta, M., and Wang, Y. *Journal of Scientific Computing* 54:454–491 (2013).
[19] Li, G., Lian, Y., Guo, Y., Jemison, M., Sussman, M., Helms, T., and Arienti, M. *International Journal for Numerical Methods in Fluids* 79:456–490 (2015).
[20] Weymouth, G. D. and Yue, D. K.-P. *Journal of Computational Physics* 229:2853–2865 (2010).
[21] Bnà, S., Cervone, A., Le Chenadec, V., and Sandro, M. In 11th International Conference of Numerical Analysis and Applied Mathematics 2013, ICNAAM 2013, Rhodes, Greece, volume 1558, 875–878 (2013).
[22] Harvie, D. J. E. and Fletcher, D. F. *Journal of Computational Physics* 162(1):1–32 (2000).
[23] Rider, W. J. and Kothe, D. B. *Journal of Computational Physics* 141(2):112–152 (1998).
[24] Smolarkiewicz, P. K. *Monthly Weather Review* 110:1968–1983 (1982).